

Research on Stability and Prevention Measures of Weathered Deposit Slope

Xiaodong Fu

¹State Key Laboratory of Geomechanics and Geotechnical Engineering, Institute of Rock and Soil Mechanics, Chinese Academy of Sciences, Wuhan, Hubei 430071, China

²University of Chinese Academy of Sciences, Beijing 100049, China

xd fu@whrsm.ac.cn

Dongge Chen

Central Yunnan Provincial Water Diversion Project Co., Ltd., Kunming, Yunnan 650051, China

Hongru Mei

Wuhan University of Engineering Science, Wuhan, Hubei 430200, China

Kunbin Yuan

China State Construction International Investments(Hubei) Limited, Wuhan, Hubei 430071, China

Wenjie Du*

¹State Key Laboratory of Geomechanics and Geotechnical Engineering, Institute of Rock and Soil Mechanics, Chinese Academy of Sciences, Wuhan, Hubei 430071, China

²University of Chinese Academy of Sciences, Beijing 100049, China

*Corresponding author: 1079502249@qq.com

Abstract—The prevention and control of geological hazards on the slopes of weathered deposits is a hot and difficult issue in the field of geotechnical engineering. According to the excavation slope characteristics of the highway in Yunnan Province, China, an engineering slope analysis model of weathered deposit body type was established, the three-dimensional finite-difference method was used to analyze the slope stability evolution law during the excavation process, and the support effect of micro-pile was studied. The research results show that, for the disturbance caused by the substep excavations, the displacement after the micro-pile support is reduced by more than 50% compared with that before the support. The research results can provide theoretical and technical support for understanding the deformation mechanism and suggesting the preventive measures for weathered deposit slope.

Keywords- deposit slope; excavation; stability; prevention measure; micro-pile

I. INTRODUCTION

According to the principle of mechanics, the prevention and control measures of highway slope can be divided into two categories [1, 2]. One is to reduce the sliding force, which is mainly realized by cutting and reducing load. The other is to improve the anti-sliding force, which is mainly through support and drainage. At present, there are three types of support ways: retaining, reinforcement and slope protection. Where, the retaining methods include anti-sliding pile, micro-pile and retaining wall; the reinforcement methods include anchor bolts and cables; slope protection methods include frame girder and plant protection [3-5].

In China, in the 1950s, drainage, cutting and load reduction, backfill and retaining wall were the main prevention and

control measures of slope. In the late 1960s, the anti-sliding pile was rapidly applied. In the late 1980s, because of fast, simple and safe construction, anchor bolts and cables were widely used; it is noted that, at this time, the prevention and control methods in practical projects were mainly drainage, supplemented by anti-sliding piles and prestressed anchor cables. In the 1990s, frame anchorage and pressure grouting can solve the problems of surface erosion and deep anti-sliding of slope. In the 21st century, the combination of active and passive support measures such as anchor cable anti-sliding pile makes the support more comprehensive and economical [6].

For improving the stability of weathered deposit slope, the slope rate method and weight reduction method are the main measures to reduce the sliding force; the mechanism of these two methods is the height and slope of slope is controlled, and the equilibrium state of sliding force and anti-sliding force of the potential sliding surface is balanced. The support ways of weathered deposit slope include retaining wall, anti-sliding pile, micro-pile and anchor engineering [7, 8]. The micro-pile, with a diameter of $\Phi 70\sim 300\text{mm}$, is constructed by placing reinforcement cage in drilling hole and then pressure grouting. By pouring the cement slurry, integrated the pile and the surrounding soil into an entity, the sliding mass is reinforced by connecting the bedrock below the sliding surface through the piles. In recent years, the micro-piles have been widely used for the advantages such as convenience of construction, less environmental impact and lower economical costs [9, 10].

In this paper, according to the characteristics of slope along the highways in Yunnan Province, China, combined with variety of prevention and control measures, the stability analysis model of weathered accumulation engineering slope is established; regarding the reliability of prevention measures for

high-risk excavated slope, the control effect during the excavation is studied by using the three-dimensional finite difference method.

II. GENERALIZED MODEL OF WEATHERED ACCUMULATION SLOPE

A generalized model of weathered accumulation slope with sedimentary rock as the bedrock is established combined with the characteristics of more than 450 slopes and landslides in Yunnan Province. The numerical model was established in FLAC 3D, which was divided into 13354 nodes and 11640 elements, as shown in Fig. 1; The model extends 80m in the X direction and 40m in the Y and Z directions; In the study area, there are three kinds of stratum: bedrock, moderately weathered layer and accumulation layer. The mechanical parameters of each stratum are shown in Table 1. The excavation of highway slope is divided into four steps from the top to bottom, and the slope ratio of each stage is 1: 0.75, as shown in Fig. 2.

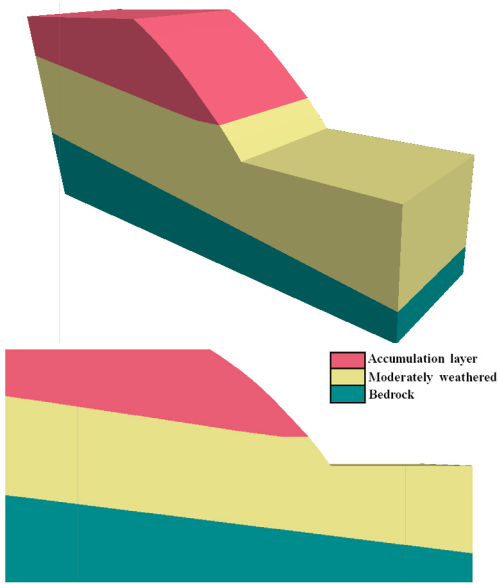


Fig. 1 Numerical model of typical generalized slope

Table 1 Physical and mechanical parameters of the geomaterials

| Stratum | Density (kg/m ³) | Cohesion (kPa) | Friction angle (°) | Yang's modulus (MPa) | Possion ratio | Bulk modulus (Pa) | Shear modulus (Pa) |
|----------------------------|------------------------------|----------------|--------------------|----------------------|---------------|---------------------|---------------------|
| Accumulation layer | 2000 | 100 | 25 | 100 | 0.35 | 1.11e ⁸ | 3.70e ⁷ |
| Moderately weathered layer | 2200 | 480 | 42 | 1920 | 0.30 | 1.60e ⁹ | 7.35e ⁸ |
| Bedrock | 2550 | 22000 | 50 | 35000 | 0.22 | 2.08e ¹⁰ | 1.43e ¹⁰ |

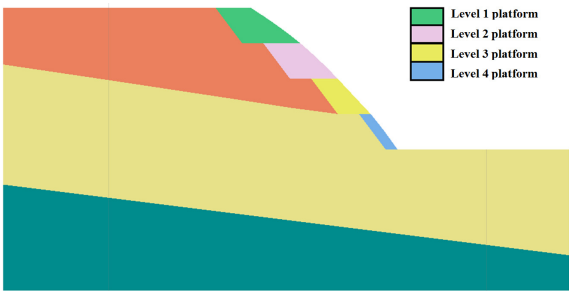
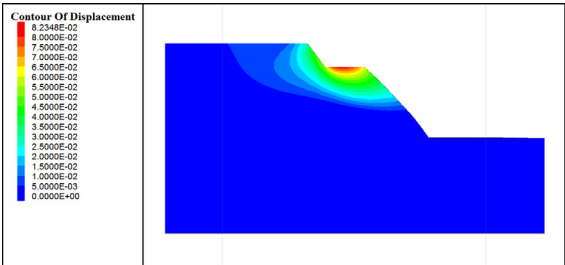


Fig. 2 Excavation steps of the slope

III. EVOLUTION OF SLOPE DEFORMATION UNDER THE STEP-BY-STEP EXCAVATION

Fig. 3 shows the contour and the vector map of the displacement field of slope during the excavation. After the first step of excavation, the maximum displacement occurs at the level 1 excavation platform, reached 76mm; the displacement around the toe of the slope is up to 54mm, while the displacement at the top of the slope is slightly small, but also reaches 32mm. After the second step of excavation, the maximum displacement is now at the level 2 excavation platform and reaches 83mm; the displacement at the toe of

level 2 excavation platform is slightly greater than that of level 1, about 57mm. After the third step of excavation, the maximum displacement occurs at the top of level 2 excavation platform, around 81mm; After the fourth step of excavation, the maximum displacement still appears at the top of level 2 excavation platform, about 80mm; It can be seen that on the level 1 and 2 excavation platform, which is the accumulation layer, the deformation is greater. Therefore, the slope during the excavation process is not stability, the slope should be reinforced.



(a) The first step of excavation

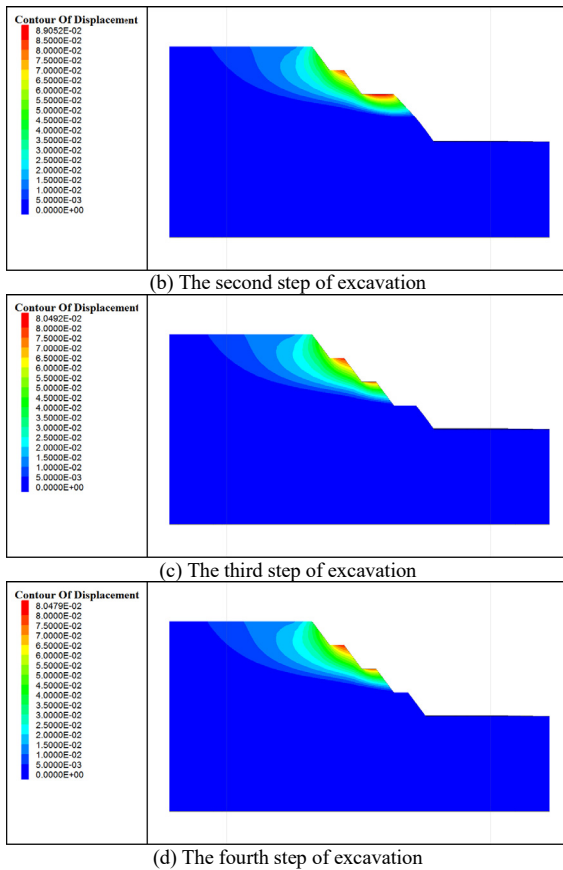


Fig. 3 The contour and the vector map of the deformation field of slope

IV. CONTROL EFFECT OF SLOPE REINFORCED BY MICRO-PILE

A. Prevention measures

Regarding to the large deformation at the level 1 and level 2 excavation platform of slope during the excavation, the micro-piles is set on the above position. The grouting micro steel tube-piles are arranged as plum blossom shape, the diameter of drilling hole is 300mm, and the pile spacing and row spacing are both 1m; A total of 5 rows piles are arranged on the top of slope, the pile length is 21m; Four rows are arranged along the slope, with different pile length but the depth of pile bottom is consistent with the piles arranged on the slope top; Three rows of micro-piles with a length of 16m are set on the level 1 excavation platform; Other three rows of micro-piles with a length of 16m are set on the level 2 excavation platform. The arrangement prevention measures are shown in Fig. 4, and the parameters of piles are shown in Table 2.

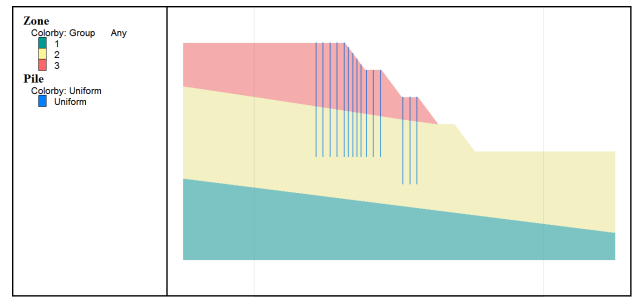


Fig. 4 Arrangement of micro-piles

Table 2 Structural element parameters

| Parameters | Value |
|--|-----------------------|
| Diameter (m) | 0.30 |
| Young's modulus (KPa) | 3.15×10^{10} |
| Poisson's ratio | 0.20 |
| Cross-sectional area (m ²) | 7.07×10^{-2} |
| second moment with respect to pile y-axis (m ⁴) | 3.98×10^{-4} |
| second moment with respect to pile z-axis (m ⁴) | 3.98×10^{-4} |
| polar moment of inertia (m ⁴) | 7.95×10^{-4} |
| normal coupling spring cohesion (N/m) | 50 |
| normal coupling spring friction angle (°) | 50 |
| normal coupling spring stiffness per unit length (N/m ²) | 8×10^{10} |

B. Deformation analysis of micro-pile

The horizontal displacement field of the micro-pile after the excavation is shown in Fig. 5. It can be seen that the maximum deformation on the top of pile reaches 42mm; Under the action of sliding force, the 9 rows of micro-piles on the top of the slope are inclined forward obviously, in which the deformation on the pile's top is the largest, the deformation of the piles gradually decreased to the depth of the slope, and the deformation tends to 0 mm at the pile's bottom. The pile deformation on level 2 platform is smaller than that of level 1 platform, slope top and slope, which is due to the greater downward sliding displacement near level 1 platform.

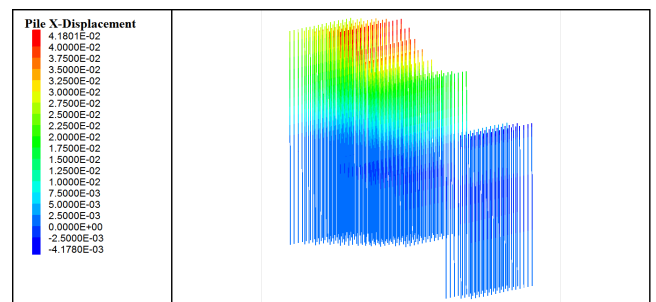


Fig. 5 Deformation contour of micro-pile after excavation

C. Effect analysis of prevention and control measures

Fig. 6 shows the displacement contour of slope after each excavation step under the support of micro-pile. The results show that after the first step of excavation, the maximum displacement at the foot of the reinforced slope is reduced from 54mm (unsupported condition) to 6mm. The displacement on the level 1 excavation platform is reduced from 76mm to

10mm. However, the displacement on the level 2 excavation platform is maintained at 62mm since no prevention measures are set on this level. After the second step of excavation, the maximum displacement at the foot on the level 2 excavation platform is reduced from 57mm (unsupported condition) to 16mm, the maximum displacement of the level 3 excavation platform is maintained at 75mm without setting any prevention measures. It follows that the micro steel tube-piles play a role and stabilized the level 1 and 2 platforms.

After the third step of excavation, the maximum displacements on level 1 and 2 excavation platforms are less than 20mm, and the maximum displacement of the slope toe is less than 25mm, the maximum displacement appears at the top of level 1 excavation platform, reached 41mm. After the fourth step of excavation, the maximum displacement still appears at the top of the level 1 platform. During the third and fourth steps of excavation, although the deformation of the slope top is increase due to the larger tensile stress, the overall displacement decreases from 81mm (without supporting) to 42mm, and the micro-piles effectively controlled the deformation of slope.

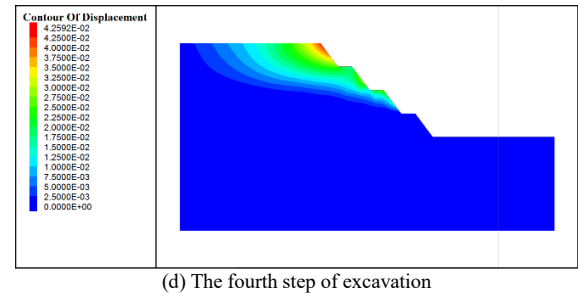
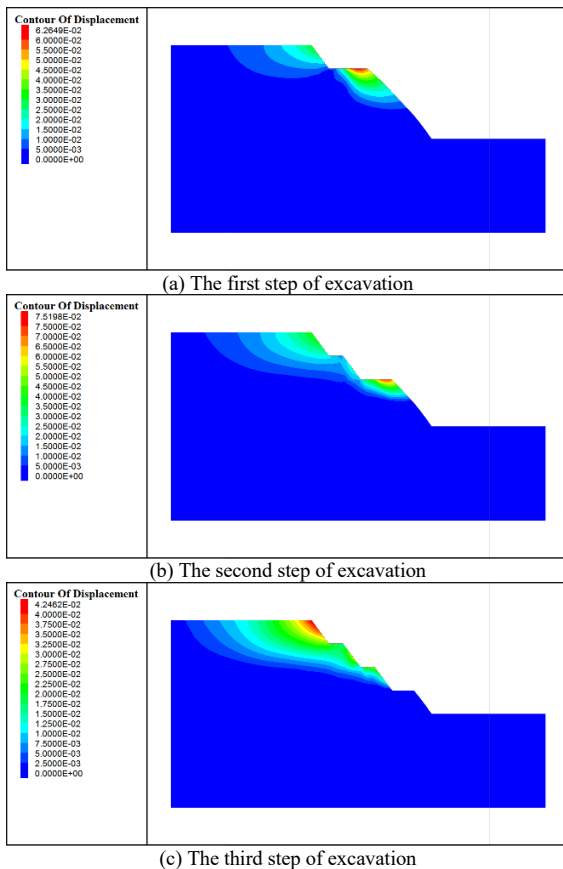


Fig. 6 Displacement contour and vector map of supported slope after excavation

Three monitoring points, hist1, hist2 and hist3, are set at the position of $x = 10\text{m}$, 20m and 30m from the boundary on the slope top, respectively; Three monitoring points, hist4, hist5 and hist6, are set at $x = 10\text{m}$, 20m and 30m on the level 1 platform. These monitoring points are used to monitor the displacement evolution during the excavation process and assessment the support effect of micro-piles, as shown in Fig. 7. It shows that the closer to the model boundary, the smaller the maximum displacement; The closer to the excavation slope top, the greater the maximum displacement; However, at the same transverse position, the maximum displacement at the level 1 platform is significantly smaller than that at the top of the slope.

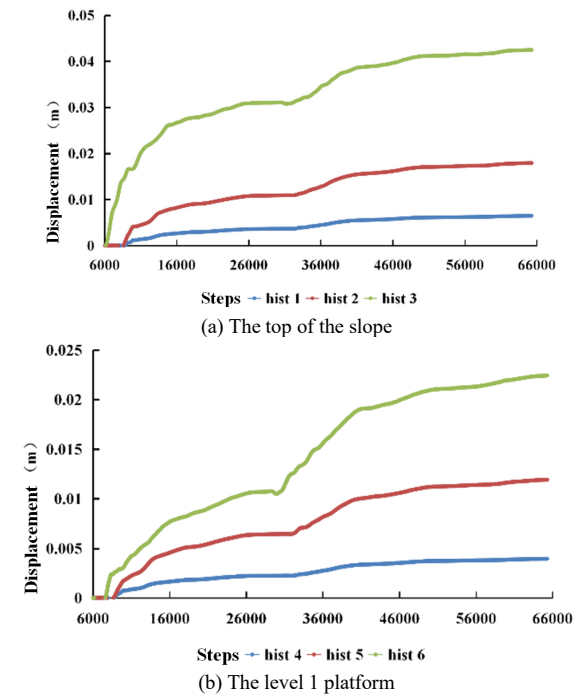


Fig. 7 Analysis of influence range of micro-pile

Four monitoring points, hist10, hist11, hist12 and hist13 are set at the slope top (i.e. $x = 30\text{m}$), $z = 40\text{m}$, 30m , 20m and 10m ; Other four monitoring points, hist14, hist15, hist16 and hist17 are set at 10m away from the slope top (i.e. $x = 20\text{m}$), $z = 40\text{m}$, 30m , 20m and 10m ; These monitoring points are used to monitor the displacement evolution during the excavation process and assessment the support effect of micro-piles, as shown in Fig. 8. It shows that at $x = 30\text{m}$ and $z = 40\text{m}$, the

displacement reaches the maximum and decreases with the decrease of elevation; the displacement at $z = 30\text{m}$ is reduced to about 50% of $z = 40\text{m}$, which shows that the micro-pile controls the displacement at the level 2 platform; At $x = 20\text{m}$, $z = 40\text{m}$, the displacement is negative, which means the displacement at this position has been obviously controlled.

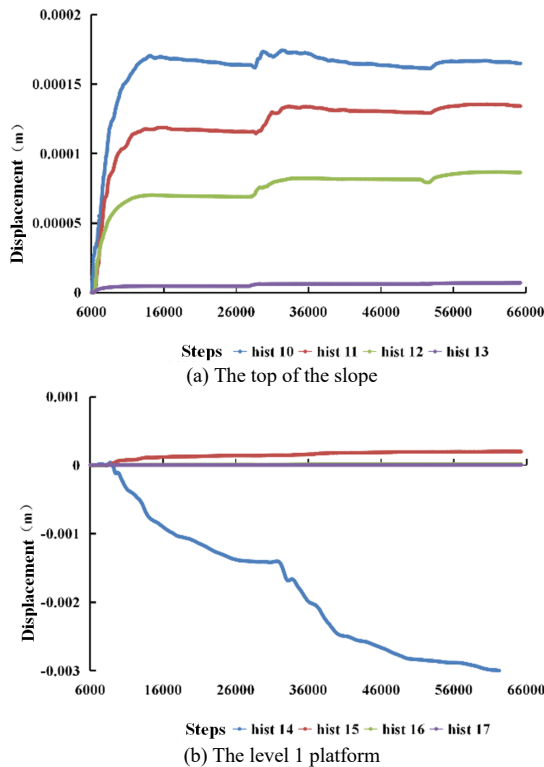


Fig. 8 Analysis of influence range of micro-pile

V. CONCLUSION

Regarding the engineering slope along highways in Yunnan Province, the stability evolution of slope in the process of excavation is analyzed. The micro-pile is proposed to reinforce the slope, the corresponding generalized model is established and the control effect of micro-pile is analyzed. The results show that:

(1) From the deformation field, when the slope is excavated without support, the maximum deformation increases gradually with the excavation steps. After the excavation, the maximum displacement appears at the level 2 and 3 excavation platform, reaching 81mm. It can be seen that the excavation disturbance has led to a partial failure of the slope.

(2) When the excavation of slope is carried out under the supporting of micro-pile, the micro-pile reduces the deformation by at least 50% and up to 86%, which indicated that the micro-pile can effectively control the slope stability under the excavation disturbance.

ACKNOWLEDGMENT

The work reported in this paper is financially supported by the National Natural Science Foundation of China (No. 52179117), the International Partnership Program of Chinese Academy of Sciences (No. 131551KYSB20180042), the Youth Innovation Promotion Association CAS (No.2021325), and the Science and Technology R&D Project of China State Construction International Holdings Limited (No. CSCI-2020-Z-21).

REFERENCES

- [1] Z.P. Zhang, X.D. Fu, Q. Sheng, and Y.X. Du, Stability of cracking deposit slope considering parameter deterioration subjected to rainfall. *International Journal of Geomechanics*, 2021, 21(7). [https://doi.org/10.1061/\(ASCE\)GM.1943-5622.0002045](https://doi.org/10.1061/(ASCE)GM.1943-5622.0002045)
- [2] G. C. Kang, Y. S. Song, and T. H. Kim, Behavior and stability of a large-scale cut slope considering reinforcement stages. *Landslides*, 2009, 6(3): 263–272.
- [3] S. G. Xiao, and J. Yang, Internal forces of double-row pile slope stabilization systems influenced by of pile row separation. *Advanced Materials Research*, 2010, 168-170: 127-132.
- [4] Z. Bo, Y. S. Wang, W. Yu, and S. Tong, Retaining mechanism and structural characteristics of h type anti-slide pile (hTP pile) and experience with its engineering application. *Engineering Geology*, 2017, 222: 29-37.
- [5] J. Xu, and F. Niu, Safety factor calculation of soil slope reinforced with piles based on Hill's model theory. *Environmental Earth Sciences*, 2014, 71(8): 3423-3428.
- [6] Y. Luo, and M. L. Xiao, Stability analysis for pre-reinforced piles within high cutting slope. *European Journal of Environmental and Civil Engineering*, 2020, (3): 1-13.
- [7] Z. P. Zhang, X. D. Fu, Q. Sheng, and, Y. X. Du, Stability of Cracking Deposit Slope Considering Parameter Deterioration Subjected to Rainfall. *International Journal of Geomechanics*, 2021, 21(7). [https://doi.org/10.1061/\(ASCE\)GM.1943-5622.0002045](https://doi.org/10.1061/(ASCE)GM.1943-5622.0002045).
- [8] X. D. Fu, Q. Sheng, W. J. Du, H. R. Mei, H. Chen, and Y. X. Du, Evaluation of dynamic stability and analysis of reinforcement measures of a landslide under seismic action: a case study on the Yanyangcun landslide. *Bulletin of Engineering Geology and the Environment*, 2020, 79: 2847–2862.
- [9] I. Juran, A. Benslimane, D.A. Bruce, Slope stabilization by micropile reinforcement. *Landslides*, 1996. 5: 1718-1726.
- [10] H. He, and Y. B. Liu, Analysis of numerical simulation of micropiles reinforcing shallow landslide. *Advanced Materials Research*, 2012, 446-449:2663-2666.